Phase-locking phenomena and excitation of damped and driven nonlinear oscillators

2009 J. Phys. A: Math. Theor. 42 045502

(http://iopscience.iop.org/1751-8121/42/4/045502)

IOP PUBLISHING JOURNAL OF PHYSICS A: MATHEMATICAL AND THEORETICAL

J. Phys. A: Math. Theor. **42** (2009) 045502 (14pp) doi:10.1088/1751-8113/42/4/045502

Phase-locking phenomena and excitation of damped and driven nonlinear oscillators

A G Shagalov[1], J Juul Rasmussen[2] and V Naulin[2]

[1] Institute of Metal Physics, Ekaterinburg 620041, Russia
[2] Risø-DTU, Building 128, PO Box 49, DK-4000 Roskilde, Denmark

E-mail: shagalov@imp.uran.ru, jens.juul.rasmussen@risoe.dk and volker.naulin@risoe.dk

Received 11 April 2008, in final form 5 November 2008
Published 19 December 2008
Online at stacks.iop.org/JPhysA/42/045502

Abstract
Resonant phase-locking phenomena ('autoresonance') in the van der Pol–Duffing oscillator forced by a small amplitude periodic driving with slowly varying frequency have been studied. We show that autoresonance occurs for oscillators with sufficiently small damping, when the system may have bi-stable states. We find the range of parameters of the oscillator, the thresholds and the appropriate control paths where autoresonant excitation of high amplitude oscillations is possible.

PACS numbers: 05.45.Xt, 52.36.Mw

1. Introduction

The phase-locking phenomena for a nonlinear pendulum with a small periodic driving were first studied in [1, 2] as a model for the acceleration of relativistic particles. The main idea of the approach is to drive the oscillator by a periodic forcing with a slowly chirping frequency in the vicinity of resonance. If the amplitude of the drive exceeds some threshold value, the phase of the oscillations can be locked by the driver, which allows us to effectively excite and control the oscillator via slow variation of the driving frequency. Resonant phase-locking phenomena (also referred to as 'autoresonance') are to date widely applied to various physical problems, which are associated with nonlinear oscillators. A wide range of applications, including plasmas and planetary dynamics is discussed by Fajans and Friedland [3]. The approach has been extended to infinite-dimensional systems, such as vortex dynamics [4] and nonlinear waves [5]. In a magnetized plasma it was demonstrated that externally excited oscillations via the phase-locking mechanism are effective in controlling various instabilities, e.g., the current driven instability [6], flute type instabilities [7] and drift wave instabilities [8]. In the first two mentioned cases the dynamics and phase locking was well described by the forced van der Pol equation. The approach may alternatively be used to the recently studied methods of control

of dissipative oscillators (see, e.g., [9]). A similar problem without driving, but with chirping of the main frequency was addressed by Meerson and Shinar [10].

In spite of the extensive studies of ODE's with slowly varying parameters (see, e.g., the recent review [11]) the problems of the phase locking by an external driving and the associated threshold phenomena are far from being solved. So far most investigations of the autoresonance have dealt with dissipationless problems. The paper of Chirikov [12] at first gives an adequate theory for the thresholds needed for phase locking to occur in the driven nonlinear pendulum. The modern mathematical aspects of this problem have been investigated in [13, 14]. Nevertheless, it has been anticipated [15, 16] that a small linear dissipation will preserve the main features of the autoresonance, but generally no expression for the threshold was proposed. However, for a dissipative system applied to plasma oscillations, discussed in [17], the threshold for autoresonance was estimated and was found to be in good agreement with experimental observations.

In the present work we focus on qualitative studying and detailed numerical simulation of the phase-locking phenomena in damped and driven systems. We base our investigation on the van der Pol–Duffing oscillator

$$\ddot{u} + u + \mu u^3 - \gamma(1 - \sigma u^2)\dot{u} = 2\epsilon \cos \Psi \tag{1}$$

driven by a small periodic forcing with amplitude $\epsilon \ll 1$ and slowly varying frequency

$$\dot{\Psi} = 1 + \Lambda(t). \tag{2}$$

We will assume a linear chirp of the frequency

$$\Lambda(t) = \alpha t.$$

In equation 1, the parameter γ designates the linear growth or dissipation rate depending on the sign, $\mu(>0)$ is the nonlinear frequency shift and $\sigma(>0)$ is a nonlinear dissipation. The slow variation implies $\mathrm{d}\Lambda/\mathrm{d}t = \alpha \ll 1$. Additionally, we assume that the parameters μ, γ and $\gamma\sigma$ are small.

2. Averaged equations

Let us introduce new variables

$$u(t) = A(t)\cos(t + \phi(t)), \qquad \dot{u}(t) = -A(t)\sin(t + \phi(t)), \tag{3}$$

where the amplitude A and the phase ϕ are supposed to be slow functions of time in accordance with the assumption of smallness of parameters in the basic equations (1)–(2). The standard averaging method [18] provides equations for the new variables

$$\dot{A} = \frac{1}{8}\gamma A(4 - \sigma A^2) - \epsilon \sin \Phi, \tag{4}$$

$$\dot{\Phi} = -\Lambda(t) + \frac{3}{8}\mu A^2 - \frac{\epsilon}{A}\cos \Phi. \tag{5}$$

Equations (4) and (5) are the generalizations of the so-called 'principal resonance equations' [19], which are the main object of study in autoresonant theory [3, 13, 14], to the van der Pol–Duffing system. The phase $\Phi(t)$ in equations (4)–(5) is the difference between the phase of the solution (3) and the forcing:

$$\Phi = \phi(t) - \int^t \Lambda(t)\,\mathrm{d}t. \tag{6}$$

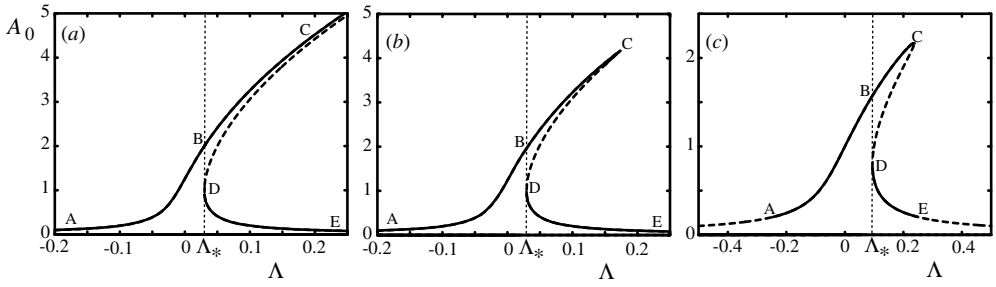

Figure 1. The amplitude A_0 of stationary solutions of the averaged equations as functions of the frequency Λ. (*a*) $\mu = 0.0267$, $\gamma = 0$, $\epsilon = 0.02$; (*b*) $\mu = 0.0267$, $\gamma = -0.0096$, $\sigma = 0$, $\epsilon = 0.02$; (*c*) $\mu = 0.134$, $\gamma = 0.0008$, $\sigma = 50$, $\epsilon = 0.05$.

Now let the frequency shift Λ be a constant. Then, equations (4)–(5) have stationary points $(A_0(\Lambda), \Phi_0(\Lambda))$ defined by the equations

$$\frac{1}{8}\gamma A_0\left(4 - \sigma A_0^2\right) - \epsilon \sin \Phi_0 = 0, \tag{7}$$

$$-\Lambda + \frac{3}{8}\mu A_0^2 - \frac{\epsilon}{A_0}\cos \Phi_0 = 0. \tag{8}$$

These points give steady cycles of the original equation (1). But not all cycles are stable. We will study the stability in the framework of equations (4)–(5). Introducing small perturbations of a stationary point $A = A_0 + \delta A$, $\Phi = \Phi_0 + \delta\Phi$ and supposing the dependence $\delta A, \delta\Phi \sim e^{\lambda t}$, we obtain from (4)–(5) the quadratic dispersion equation

$$\lambda^2 - \left[\frac{\epsilon}{A_0}\sin \Phi_0 + \frac{1}{8}\gamma\left(4 - 3\sigma A_0^2\right)\right]\lambda + \frac{1}{8}\gamma\left(4 - 3\sigma A_0^2\right) \times \frac{\epsilon}{A_0}\sin \Phi_0 + \epsilon \cos \Phi_0\left[\frac{3}{4}\mu A_0 + \frac{\epsilon}{A_0^2}\cos \Phi_0\right] = 0. \tag{9}$$

The steady solution (A_0, Φ_0) will be stable if $\mathrm{Re}\,\lambda \leqslant 0$.

Typical solutions, $A_0(\Lambda)$, of equations (7)–(8) are shown in figure 1, for the three different sets of parameters which will be investigated in this paper:

(a) dissipationless case, $\gamma = 0$,

(b) simplest linear dissipation, $\gamma < 0$ and $\sigma = 0$,

(c) van der Pol–Duffing case, $\gamma > 0$ and $\sigma > 0$.

We suppose that in all the cases $\alpha \geqslant 0, \mu \geqslant 0$ and $\epsilon \geqslant 0$. The solid line parts of the curves in figure 1 represent stable solutions ($\mathrm{Re}\,\lambda \leqslant 0$), and dashed lines correspond to unstable solutions ($\mathrm{Re}\,\lambda > 0$).

In the dissipationless case (a), the route to excite high amplitude oscillations in the vicinity of the line BC in figure 1(*a*) is to apply the forcing at a very low amplitude and sweep the frequency $\Lambda(t) = \alpha t$ from a negative value, i.e., to start at a large negative time t_0. It is obvious that such a result cannot be obtained by excitation with a constant frequency $\Lambda \geqslant \Lambda_*$ (Λ_* being defined in figure 1), because in this case one can attain only the low amplitude near the line DE. The appropriate controlling path has to use a slowly varying frequency (2) [3]. Starting from the time t_0 one crosses the resonance $\dot{\Psi} = 1$ at $t = 0$ and, then, forces the solution to move in the vicinity of the stable curve BC to excite a high amplitude oscillation. It is important to note, that this development can only be realized when α is less

than some critical value $\alpha_{cr} \sim \epsilon^{4/3}$ [3]. The physical mechanism of the phenomenon is the phase locking of the excited oscillations by the forcing. In the following section we study new aspects of this phenomena, which allow us to extend the phase-locking approach to dissipative systems of types (b) and (c).

The amplitude curves for the dissipative cases are shown in figures 1(*b*) and (*c*). The main difference from the previous case (where $\mathrm{Re}\,\lambda = 0$) is that now $\mathrm{Re}\,\lambda < 0$ and the stable parts of the curves associate with attractive behavior of the system (4)–(5). For any fixed Λ, a zero initial solution tends to the corresponding point $A_0(\Lambda)$ on the curve. But again, the high amplitude solutions on the curve BC are not directly attainable. One notes that in the van der Pol–Duffing case (c) the small amplitude oscillations are unstable themselves and the range of stable limit cycles are restricted to a finite interval of Λ where $A_0^2 \geqslant 2/\sigma$. It will be shown in the following that phase locking in the dissipative cases is also possible with some restrictions on the parameter α and for specific controlling paths.

It is important to note that in the dissipative cases the phase-locking approach has meaning only if the function $A_0(\Lambda)$ is multivalued in some regime, like the curve BCD in figure 1. In the dissipationless case the point C moves out to infinity. This is the case for a sufficiently small dissipation. In case (b), the exact limitation is

$$|\gamma| < \left(\tfrac{3}{2}\mu\epsilon^2\right)^{1/3}. \tag{10}$$

In case (c), the limitation is more sophisticated, but the simplified sufficient condition reads

$$\gamma \ll \frac{3\mu}{\sigma}. \tag{11}$$

For larger γ the curves become single valued and any Λ corresponds to one unique value of A_0. In this case no specific control path is needed to excite high amplitude stable cycles. The simplest setup with constant Λ is sufficient to attain any admissible amplitudes.

Let us return to the dynamical equations (4)–(5). Differentiating equation (5) and eliminating $\dot{A}$ by equation (4) we obtain the equation for the phase difference, Φ between the excited oscillations and the forcing

$$\ddot{\Phi} = -\frac{\partial U}{\partial \Phi} + \Gamma\dot{\Phi}. \tag{12}$$

This resembles the equation of motion for a 'quasi-particle' with coordinate Φ located in the effective potential

$$\begin{aligned} U(A,\Phi) = &\left[\alpha - \frac{3}{32}\mu\gamma A^2(4-\sigma A^2)\right]\Phi \\ &-\frac{3}{4}\mu\epsilon A\cos\Phi - \frac{\epsilon\gamma}{8A}(4-\sigma A^2)\sin\Phi - \frac{1}{4}\frac{\epsilon^2}{A^2}\cos 2\Phi \end{aligned} \tag{13}$$

and with the dissipation coefficient

$$\Gamma(A) = -\frac{1}{A}\frac{\mathrm{d}A}{\mathrm{d}t} + \frac{1}{8}\gamma(4-\sigma A^2). \tag{14}$$

These equations contain the amplitude A as a parameter. One can see that the potential U may have minima in some range of A if the forcing has a sufficiently large amplitude ϵ. In this case the 'quasi-particle' can be trapped in a potential well, which implies, in accordance with the definition (6), that the phase difference between forcing and excited oscillations is bounded, i.e., the oscillations are phase locked. Thus, the existence of minima in the effective potential (13) is a necessary condition for phase locking. It becomes sufficient only for appropriate initial conditions in (4)–(5), which then constrains the system to be phase locked.

3. Oscillator without dissipation

When $\gamma = 0$, the minima of the effective potential (13) are located in points where

$$\frac{\mathrm{d}U}{\mathrm{d}\Phi} = \alpha + \left(\frac{9}{32}\mu A + \frac{\epsilon}{A^2}\cos\Phi\right)\epsilon\sin\Phi = 0. \tag{15}$$

Because the variation of the amplitude A is not limited in this case (see figure 1(a)), we have to find a sufficient condition for the existence of the minima for any A.

There is a minimum in some range $[\Phi_1, \Phi_2]$, if $\mathrm{d}U/\mathrm{d}\Phi$ has different signs at $\Phi = \Phi_1$ and $\Phi = \Phi_2$. That is the following two inequalities should hold:

$$\alpha + \epsilon\left(\frac{9}{32}\mu A + \frac{\epsilon}{A^2}\cos\Phi_1\right)\sin\Phi_1 < 0, \tag{16}$$

$$\alpha + \epsilon\left(\frac{9}{32}\mu A + \frac{\epsilon}{A^2}\cos\Phi_2\right)\sin\Phi_2 > 0. \tag{17}$$

It is obvious that the inequality (17) has solutions $\Phi_1 \in (0, \pi/2)$ for any $A > 0$.

To consider (16) we introduce the function

$$f(\Phi, A) = -\epsilon\left(\frac{9}{32}\mu A + \frac{\epsilon}{A^2}\cos\Phi\right)\sin\Phi. \tag{18}$$

For a given $A > 0$, f is bounded as a function of Φ. The inequality (16) certainly will have solutions if

$$\alpha < \max_{\Phi} f(\Phi, A) = F(A). \tag{19}$$

The maximum value of (18) will be at

$$\cos\Phi = \cos\Phi_+ = -\frac{3\mu}{16\epsilon}A^3 + \sqrt{\left(\frac{3\mu}{16\epsilon}\right)^2 A^6 + \frac{1}{2}} \tag{20}$$

and, thus,

$$F(A) = f(\Phi_+, A). \tag{21}$$

The function $F(A)$ tends to infinity at $A \to 0$ and $A \to \infty$ and have a minimum at $A^3 = 4\epsilon/3\mu$. Then, we have the sufficient condition for which the effective potential (13) has minima for all $A > 0$:

$$\begin{aligned}\alpha < \alpha_{\mathrm{cr}} = F([4\epsilon/3\mu]^{1/3}) &= \frac{3^{13/6}}{2^{10/3}}\mu^{2/3}\epsilon^{4/3} \\ &\approx 1.072\mu^{2/3}\epsilon^{4/3}.\end{aligned} \tag{22}$$

In the opposite case, when the threshold condition (22) is violated, $\alpha > \alpha_{\mathrm{cr}}$, there is a finite gap $[A_1, A_2]$ where the effective potential has no minima.

The dynamics of the system is shown in figures 2 and 3 for two different initial conditions. We use the linear dependence $\Lambda(t) = \alpha t$ and distinguish initial conditions by the starting times: $t_0 = -400$ and $t_0 = 0$. In both cases we used $A = 0.001$ and $\dot{\Phi} = 0$ at the starting point $t = t_0$. The latter condition implies $\Phi(t_0) \approx -\pi/2$ and follows from the requirement that the solutions of (4)–(5) should be slow in time. Initial conditions for equation (1) were adjusted with (4)–(5) according to the relation (3). The original equation (1) has no restrictions of the phase $\Phi(t_0)$. We have checked numerically that the results did not depend on the initial phase in both cases if the initial amplitude is small enough.

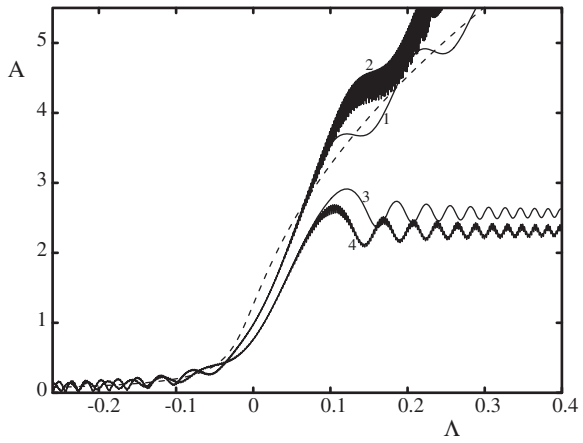

Figure 2. Dynamics of the system (4)–(5) (lines 1 and 3) and equation (1) (lines 2 and 4) for linear dependence of the forcing frequency $\Lambda(t) = \alpha t$ at $t \geqslant t_0 = -400$. $\mu = 0.0267$, $\gamma = 0$, $\epsilon = 0.02$. Lines 1 and 2 – $\varkappa = 1.342$ ($\alpha = 0.00065$); lines 3 and 4 – $\varkappa = 1.754$ ($\alpha = 0.00085$) ($\varkappa$ is defined in equation (23)). The dashed line is the curve ABC from figure 1(*a*).

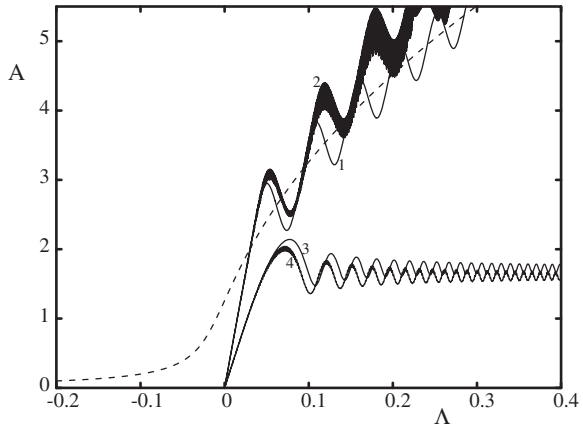

Figure 3. Dynamics of the system (4)–(5) (lines 1 and 3) and equation (1) (lines 2 and 4) for linear dependence of the forcing frequency $\Lambda(t) = \alpha t$ at $t \geqslant t_0 = 0$. $\mu = 0.0267$, $\gamma = 0$, $\epsilon = 0.02$. Lines 1 and 2 – $\varkappa = 0.619$ ($\alpha = 0.0003$); lines 3 and 4 – $\varkappa = 1.094$ ($\alpha = 0.00053$). Dashed line is the line ABC from figure 1(*a*).

The first case, when $t_0 = -400$ (see figure 2), is associated with the control path used in [3]. Lines 1 and 2 show the dynamics of the systems (4)–(5) and (1), respectively, when α is sufficiently small. The amplitude grows infinitely fluctuating around the dashed curve, which is the curve ABC in figure 1(*a*). For equation (1), we use the value $\sqrt{u^2 + \dot{u}^2}$ as the amplitude of oscillations, corresponding to the transformation in (3). The 'thickness' of line 2 (the solution to equation (1)), owing to high frequency fluctuations, is caused by the difference between the proposed circular orbits (3) and the real ones, which is appreciable for high amplitudes. A similar growth of the amplitude has been observed earlier, see, e.g., [3], where it was shown to be the result of the phase locking (the 'autoresonance' effect). In contrast,

when α exceeds some threshold value, the amplitude is saturated (lines 3, 4) at a small level and high amplitudes associated with the range BC in figure 1 becomes unattainable. A quite similar behavior has been observed in the second case when the initial time is $t_0 = 0$, see figure 3.

It is convenient to characterize the threshold phenomena by the dimensionless parameter

$$\varkappa = \frac{\alpha_{\rm cr}}{\mu^{2/3}\epsilon^{4/3}}. \tag{23}$$

Thus, the threshold value, found analytically in (22), corresponds to $\varkappa = 1.072$. The threshold value found numerically for the system (4)–(5) for $t_0 = -400$ is

$$\varkappa \approx 1.696, \tag{24}$$

and for the original equation (1) it is $\varkappa \approx 1.531$. In the second case, when $t_0 = 0$, the critical value is found to be

$$\varkappa \approx 1.009 \tag{25}$$

for the system (4)–(5) and $\varkappa \approx 0.950$ for the original equation (1).

We note that the same threshold as in (24) was found in [20]. It is larger then the value $\varkappa = 1.072$ found analytically. On the other hand, for $t_0 = 0$, the critical value (25) is rather close to the analytical value. To comprehend these results we should analyze the evolution of the phase $\Phi(t)$ for the system (4)–(5). This is shown in figure 4, where trajectories $(\Phi(t), A(t))$ of the solutions are plotted and related to the location of extremum points of the effective potential $U(A, \Phi)$ (13). The dashed lines in the figures are the locations where $U(A, \Phi)$ has minima in the (A, Φ)-plane. The dotted lines indicate maxima of the potential. In figures 4(a) and (b) $\varkappa$ is greater than the analytical value 1.072, thus there are gaps where the potential has no extremum points. In contrast, in figure 4(c), the parameter $\varkappa < 1.072$ and the potential has the extremum points in the whole range of A-values. The trajectories $(\Phi(t), A(t))$ shown in figures 4(a) and (b) represent the dynamics of the solutions in another way than the curves 1 and 3 in figure 2. The main features of the dynamics are: in the initial stage of the process ($t < 0$), before crossing the resonance, the system is phase locked in the potential mimimum near $\Phi = 0$. It provides a high probability to overcome the gaps, where no extrema exist. If $\varkappa < 1.696$ (see figure 4(a)), the gap is not too wide and the system can successfully overcome the gap and then phase lock in the minimum of the potential at high amplitudes. This is reflected in figure 2 as infinite growth of the amplitude (line 1). In the opposite case, when $\varkappa > 1.696$ (see figure 4(b)), the gap is so wide that the system, even being phase locked at the initial stage, cannot be captured in the potential minimum at the high amplitudes after passing the gap. Phase locking is then destroyed and saturation of the excitation is observed (line 3, figure 2). It appears obvious that phase locking at the initial stage causes an appropriate preparation of the system to overcome the gap, which explains the observed increase of the critical value above the theoretical limit (22).

In the second case, at $t_0 = 0$, the system starts just at the resonance (figure 3). There is no initial phase locking and the trajectory starts near the unstable region of maximum of the potential (at $\Phi \approx -\pi/2$, see figure 4(c)). In this case the dynamics becomes very sensitive to the structure of the effective potential. The potential should have a global minimum for any A in order that the 'quasi-particle' can be trapped—the oscillations phase locked. As a result we observe the threshold (25) to be close to the analytical value $\varkappa = 1.072$.

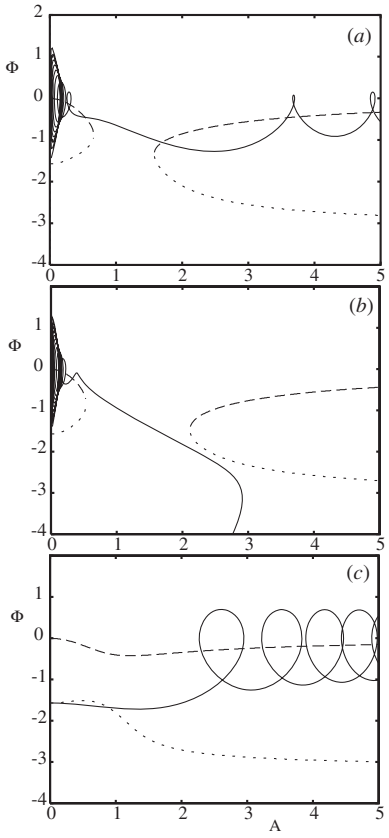

Figure 4. The trajectories $(\Phi(t), A(t))$ of the system (4)–(5) (solid lines) at $\mu = 0.0267, \gamma = 0, \epsilon = 0.02$. (*a*) $t_0 = -400, \varkappa = 1.342$ ($\alpha = 0.00065$); (*b*) $t_0 = -400, \varkappa = 1.754$ ($\alpha = 0.00085$); (*c*) $t_0 = 0, \varkappa = 0.619$ ($\alpha = 0.0003$). Dashed lines—minima of the effective potential $U(\Phi, A)$ at fixed A; dotted lines—maxima of the effective potential.

4. Oscillator with linear dissipation

The minima of the effective potential for the oscillator with $\gamma < 0$ and $\sigma = 0$ are defined by the equation

$$\frac{\mathrm{d}U}{\mathrm{d}\Phi} = \alpha + \left(\frac{3}{4}\mu A + \frac{\epsilon}{A^2}\cos\Phi\right)(\epsilon\sin\Phi - 4\gamma A) = 0. \tag{26}$$

As in the previous section we introduce the auxiliary function $F(A) = \max_\Phi f(\Phi, A)$, where

$$f(\Phi, A) = -\epsilon\left(\frac{3}{4}\mu A + \frac{\epsilon}{A^2}\cos\Phi\right)\left(\sin\Phi - \frac{\gamma A}{2\epsilon}\right). \tag{27}$$

The sufficient condition for the potential to have minima takes the form

$$\alpha < F(A). \tag{28}$$

The typical form of the function $F(A)$ is shown in figure 5. It tends to infinity at $A \to 0$ and becomes zero, when the amplitude achieves the maximum value at the point C: $A = A_C$ (see figure 1(*b*)). In contrast to the dissipationless case, the function $F(A)$ has no absolute

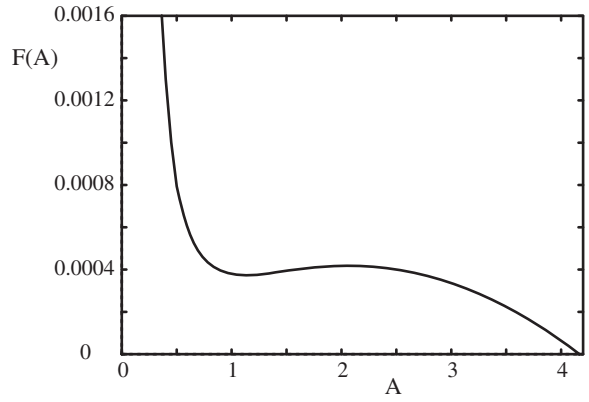

Figure 5. The auxiliary function $F(A)$ for $\mu = 0.0267, \gamma = -0.0096, \sigma = 0, \epsilon = 0.02$.

minimum and the condition (28) will define only a range of amplitudes where the effective potential can have minima. It is seen from figure 5 that, in the range $F(A) \gtrsim 0.0004$, the minima of the potential are possible only for small amplitudes. On the other hand, for $F(A) \lesssim 0.0004$, the possible range of the minima rapidly enlarges up to the maximum value of the amplitude, $A_C = 4.17$. Our goal of excitation is to attain amplitudes in the range of line BC (figure 1(*b*)), that is in the range $A_B = 1.96 < A < A_C = 4.17$. We propose that such excitations will only be possible if the range of minima of the potential covers high amplitudes making the phase locking available, thus the threshold condition should be

$$\alpha \lesssim 0.0004. \tag{29}$$

To test this threshold numerically we apply the following controlling path:

$$\Lambda(t) = \begin{cases} \alpha t, & t_0 < t \leqslant \Lambda_0/\alpha \\ \Lambda_0, & t > \Lambda_0/\alpha. \end{cases} \tag{30}$$

At initial times we use the linear chirping of the frequency and then, at $t > \Lambda_0/\alpha$, the chirping is switched off. The parameter Λ_0 is chosen so that the corresponding amplitude $A_0(\Lambda_0)$ lies on the curve BC (figure 1(*b*)). Because BC is the range of attractive focuses of the system (4)–(5), the path after switching off the chirping should excite a stable cycle, which is a solution of equations (7)–(8) for $\Lambda = \Lambda_0$. Figure 6 illustrates the dynamics of the system (4)–(5) using the controlling path (30), when the threshold condition (29) is fulfilled.

Using the controlling path (30) and varying Λ_0 we have studied the important problem of what maximum value one can reach for the amplitude of oscillations for a given α. The results are collected in figure 7 for $t_0 = -400$ (solid line) and $t_0 = 0$ (dashed line). The curves confirm that the proposed value (29) is a proper threshold for reaching high amplitude excitations. Especially, this is clearly observed from the case for $t_0 = 0$ (dashed line), where the attainable amplitudes undergo a jump as α crosses the critical value around 0.0004. As it was discussed in the previous section, for the initial condition with $t_0 = 0$, the dynamics of the system is very sensitive to the detailed form of the effective potential, which becomes apparent in the jump of amplitudes at the threshold.

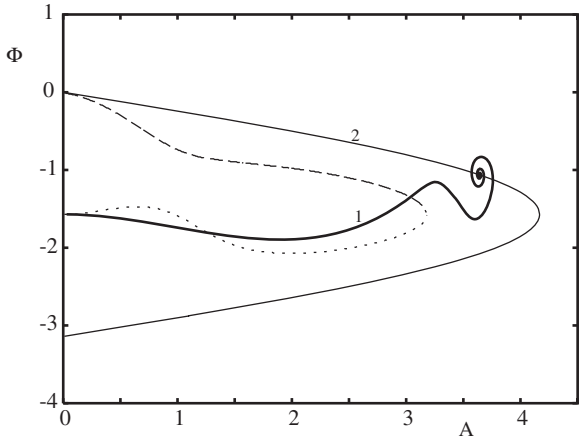

Figure 6. Dynamics of the system (4)–(5) in the plane $(\Phi(t), A(t))$ (solid line 1) under the controlling path (30) for $t_0 = 0, \Lambda_0 = 0.13$ and $\mu = 0.0267, \gamma = -0.0096, \sigma = 0, \epsilon = 0.02, \alpha = 0.0003$. Solid line 2–stationary solutions $(A_0(\Lambda), \Phi_0(\Lambda))$ of the system (7)–(8). Dashed line–minima of the effective potential $U(\Phi, A)$ at fixed A. Dotted line–maxima of the effective potential.

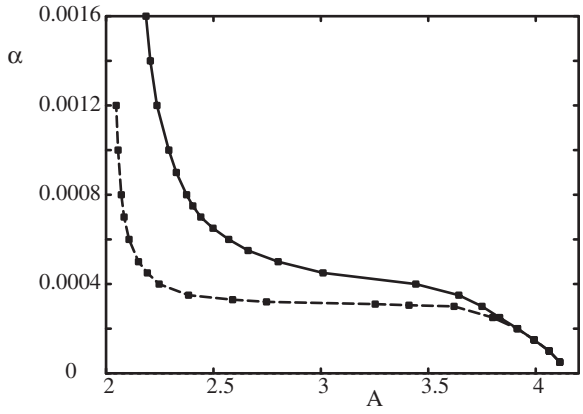

Figure 7. The maxima of the amplitude A_0 attainable at a given α. Solid line: $t_0 = -400$, dashed line: $t_0 = 0$; $\mu = 0.0267, \gamma = -0.0096, \sigma = 0, \epsilon = 0.02$.

The main characteristic of the phase-locking phenomena is the dependence of the critical value α_{cr} on the amplitude of forcing ϵ. In the dissipationless case it has the form of a power law, $\alpha_{cr} \propto \epsilon^{4/3}$. To study the dependence in the cases with dissipation we define the function

$$\alpha_0 = \min_{[0,A_0]} F(A), \tag{31}$$

where A_0 is the amplitude of the stationary solution corresponding to Λ_0 in the controlling path (30). Then we suppose that the threshold condition, when the amplitude can attain the value A_0, is

$$\alpha < \alpha_{cr} = \alpha_0. \tag{32}$$

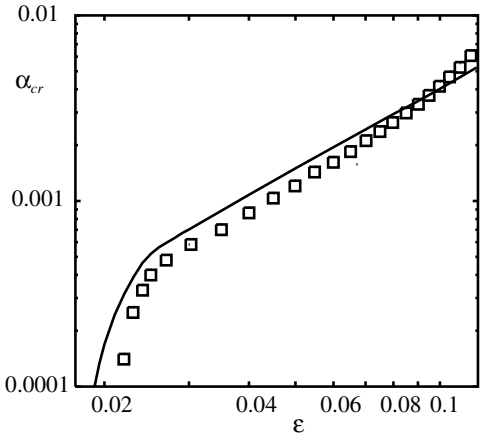

Figure 8. The dependence of the critical value $\alpha_{\rm cr}$ on the amplitude of forcing ϵ for the path (30) with $\Lambda_0 = 0.13$ and $t_0 = 0$; $\mu = 0.0267$, $\gamma = -0.0096$, $\sigma = 0$. □—equation (1), the solid line is $\alpha_{\rm cr} = \alpha_0(\epsilon)$ obtained from equation (31).

The comparison of the theoretical value of the threshold (31), (32) with computations of the original equation (1) is shown in figure 8. It is clearly observed that the behavior is more complex than the power law behavior in the dissipationless case. The numerical and analytically estimated thresholds exhibit a similar behavior except near the edges of the range studied. For small ϵ no stationary cycles are observed for the prescribed controlling path. On the other hand, for large ϵ, the numerical results defer from theoretical values, because of the violation of the conditions of smallness. We note that the results above only slightly depend on the other parameters γ and μ, while the inequality (10) is fulfilled.

5. van der Pol–Duffing oscillator

The minima of the effective potential for the oscillator with $\gamma > 0$ and $\sigma > 0$ are defined by the equation

$$\frac{{\rm d}U}{{\rm d}\Phi} = \alpha + \left(\frac{3}{4}\mu A + \frac{\epsilon}{A^2}\cos\Phi\right)(\epsilon\sin\Phi - \gamma A(4 - \sigma A^2)) = 0. \tag{33}$$

Proceeding as in the previous sections, we can find the sufficient condition for when the effective potential has minima,

$$\alpha < F(A). \tag{34}$$

For small γ (11), the typical shape of the function $F(A)$ is shown in figure 9. Like for the case with linear dissipation, $F(A)$ becomes zero when the amplitude achieves the maximum value at the point C (see figure 1(*c*)). It is seen from figure 9 that for $F(A) \lesssim 0.005$ the possible range for the existence of minima rapidly enlarge. The goal of the excitation is to attain amplitudes in the range of the line BC (figure 1(*c*)). We propose that the threshold

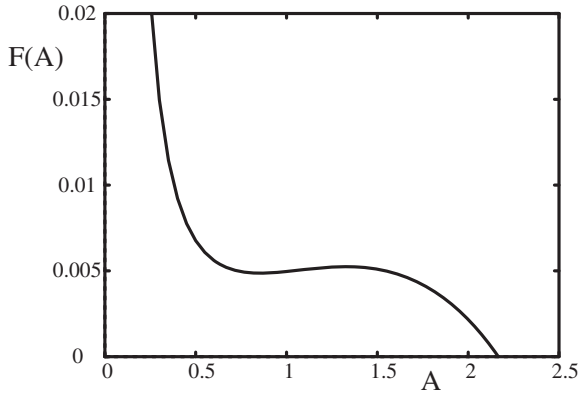

Figure 9. The auxiliary function $F(A)$ (equation (34)) for $\mu = 0.134$, $\gamma = 0.0008$, $\sigma = 50$, $\epsilon = 0.05$.

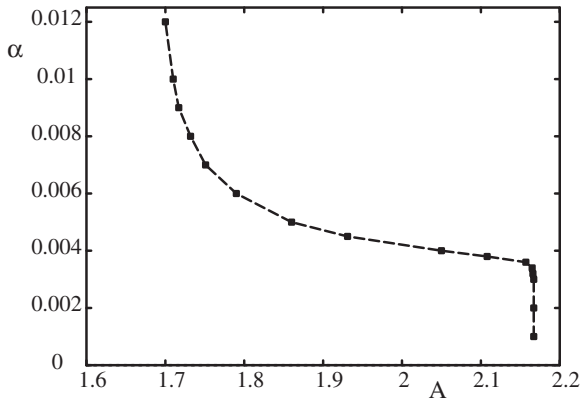

Figure 10. The maxima of the amplitude A attainable at a given α for the path (30) with $t_0 = 0$; $\mu = 0.134$, $\gamma = 0.0008$, $\sigma = 50$, $\epsilon = 0.05$.

condition should be

$$\alpha \lesssim 0.005. \tag{35}$$

This is confirmed by the numerical results collected in figure 10. We have used the controlling path (30) and varied Λ_0 to reach maximum of the amplitude of oscillations for a given α. We have only used the initial conditions with $t_0 = 0$, because the range of variation of Λ in this case is bounded to be around zero by the stability condition. One can see from the curve that the expression in equation (35) may be used as a threshold, because the line undergoes a jump as α crosses this critical value.

As in the previous section we introduce the theoretical threshold condition (31)–(32). The comparison of this value with the computations of the original equation (1) is shown in figure 11. We observe also here a behavior different from the power law behavior. For small ϵ no stationary cycles are observed and the threshold condition disappears, for large ϵ, one observes the increasing difference with analytic and numerical values.

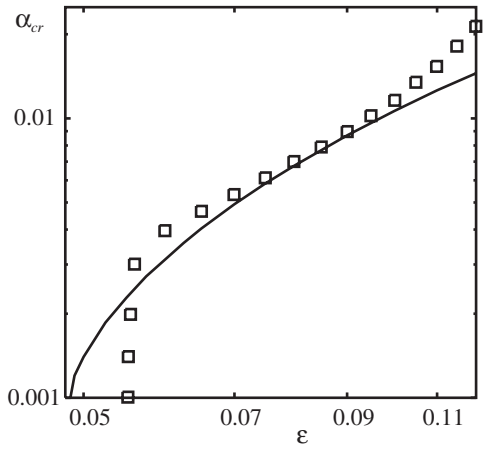

Figure 11. The dependence of the critical value $\alpha_{\rm cr}$ on the amplitude of forcing ϵ for the path (31) with $\Lambda_0 = 0.2$ and $t_0 = 0$; $\mu = 0.134$, $\gamma = 0.0008$, $\sigma = 50$. □—equation (1), the solid line is $\alpha_{\rm cr} = \alpha_0(\epsilon)$.

6. Conclusion

In this paper we have studied the excitation of high amplitude oscillations for the weakly damped and driven nonlinear pendulum by means of control of the oscillations via the phase-locking effect ('autoresonance'). The effect is based on the capture of the phase of oscillations by the external forcing with chirping frequency, when its amplitude and chirp rate obey some threshold conditions. The applied averaged approach results in studying the dynamics of some 'quasi-particle' located in an effective potential where the coordinate of the quasi-particle is the phase difference between the forcing and the oscillations. The threshold conditions are associated with the existence of global minima in the potential, where the quasi-particle could be trapped.

In the dissipationless case we have found the threshold conditions and compared them with the direct numerical solutions of the original model for two different control paths. We explained how the real thresholds can be associated with the theoretical ones taking into account the complex dynamics of the quasi-particle. We have extended the approach first to the systems with linear dissipation and then to the full van der Pol–Duffing equation. The appreciable phase-locking phenomena for the dissipative systems can be observed only for sufficiently small effects of the dissipation, when the systems may have bi-stable states. It is important that the potential minima cannot be global in these cases and the threshold conditions cover a finite range of amplitudes of excited oscillations. We have found that the dependence of the critical chirp rates on the amplitude of forcing appearing in the threshold conditions for dissipative systems exhibits more complex behavior than the power-like one in the dissipationless case.

Acknowledgment

The authors thank L Friedland for helpful discussions. The work was supported by INTAS (Grant No. 03-51-4286).

References

[1] McMillan E M 1946 *Phys. Rev.* **68** 143
[2] Veksler V I 1945 *J. Phys. USSR* **9** 153
[3] Fajans J and Friedland L 2001 *Am. J. Phys.* **69** 1096
[4] Friedland L and Shagalov A G 2002 *Phys. Fluids* **14** 3074
[5] Friedland L and Shagalov A G 2005 *Phys. Rev.* E **71** 036206
[6] Michelsen P, Recseli H L, Rasmussen J J and Schrittwieser R 1979 *Plasma Phys.* **22** 61
[7] Iizuka S, Huld T, Recseli H L and Rasmussen J J 1988 *Phys. Rev. Lett.* **60** 1026
[8] Schröder C, Klinger T, Block D, Piel A, Bonhomme G and Naulin V 2001 *Phys. Rev. Lett.* **86** 5711
Klinger T, Schröder C, Block D, Greiner F, Piel A, Bonhomme G and Naulin V 2001 *Phys. Plasmas* **8** 1961
[9] Ji J C and Hansen C H 2006 *Chaos Solitons Fractals* **28** 555
[10] Meerson B and Shinar G I 1997 *Phys. Rev.* E **56** 256
[11] Sanders J, Verhulst F and Murdock J 2007 *Averaging methods in nonlinear dynamical systems (Springer Series on Applied Mathematical Sciences vol 59)* (New York: Springer) p431
[12] Chirikov B V 1959 *Dokl. Akad. Nauk. SSSR* **125** 1015
[13] Kalykin L A 2004 *Diff. Eqns* **40** 780
[14] Maslov E M, Kalykin L A and Shagalov A G 2007 *Theor. Math. Phys.* **152** 1173
[15] Yariv S and Friedland L 1993 *Phys. Rev.* E **48** 3072
[16] Khain E and Meerson B 2001 *Phys. Rev.* E **64** 036619
[17] Fajans J, Gilson E and Friedland L 2001 *Phys. Plasmas* **8** 423
[18] Nayfeh A H 1981 *Introduction to Perturbation Technique* (New York: Wiley)
[19] Haberman R and Ho E K 1990 *J. Appl. Mech.* **62** 941
[20] Marcus G, Friedland L and Zigler A 2004 *Phys. Rev.* A **69** 013407